Tantalum oxide/silicon nitride: A negatively charged surface passivation stack for silicon solar cells

Yimao Wan, James Bullock, and Andres Cuevas

Citation: Applied Physics Letters **106**, 201601 (2015); doi: 10.1063/1.4921416

View online: http://dx.doi.org/10.1063/1.4921416

View Table of Contents: http://scitation.aip.org/content/aip/journal/apl/106/20?ver=pdfcov

Published by the AIP Publishing

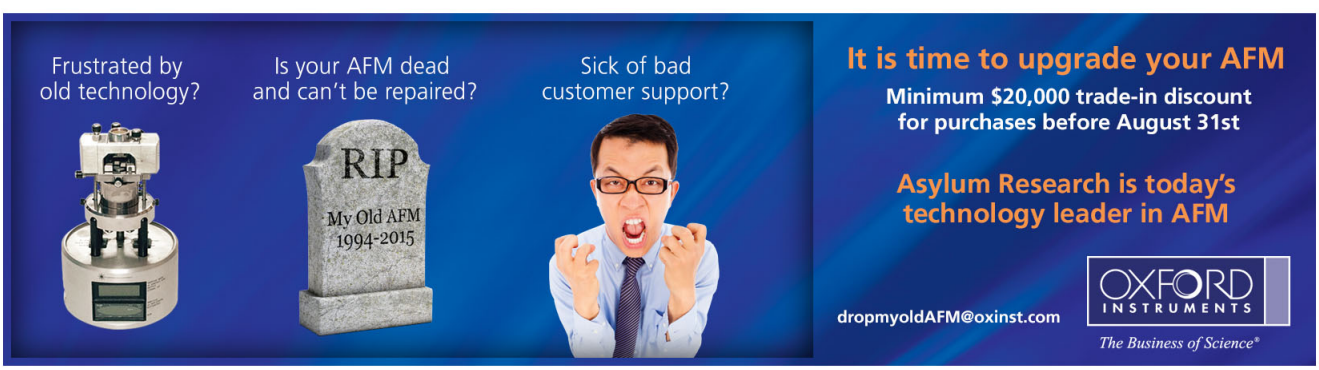

Tantalum oxide/silicon nitride: A negatively charged surface passivation stack for silicon solar cells

Yimao Wan,[a] James Bullock, and Andres Cuevas
Research School of Engineering, The Australian National University, Canberra, ACT 0200, Australia

(Received 25 February 2015; accepted 9 May 2015; published online 18 May 2015)

This letter reports effective passivation of crystalline silicon (c-Si) surfaces by thermal atomic layer deposited tantalum oxide (Ta_2O_5) underneath plasma enhanced chemical vapour deposited silicon nitride (SiN_x). Cross-sectional transmission electron microscopy imaging shows an approximately 2 nm thick interfacial layer between Ta_2O_5 and c-Si. Surface recombination velocities as low as 5.0 cm/s and 3.2 cm/s are attained on *p*-type 0.8 Ω·cm and *n*-type 1.0 Ω·cm c-Si wafers, respectively. Recombination current densities of 25 fA/cm^2 and 68 fA/cm^2 are measured on 150 Ω/sq boron-diffused p^+ and 120 Ω/sq phosphorus-diffused n^+ c-Si, respectively. Capacitance–voltage measurements reveal a negative fixed insulator charge density of -1.8×10^{12} cm^{-2} for the Ta_2O_5 film and -1.0×10^{12} cm^{-2} for the Ta_2O_5/SiN_x stack. The Ta_2O_5/SiN_x stack is demonstrated to be an excellent candidate for surface passivation of high efficiency silicon solar cells. © *2015 AIP Publishing LLC*. [http://dx.doi.org/10.1063/1.4921416]

Within crystalline silicon (c-Si) photovoltaics, trends toward lighter dopant diffusions, thinner substrates, and higher bulk lifetimes have placed an increased importance on surface passivation. An array of dielectrics have been demonstrated to effectively suppress the defect-assisted Shockley–Read–Hall recombination at the surface, most notably silicon oxide (SiO_2),[1] silicon nitride (SiN_x),[2,3] amorphous silicon (a-Si),[4] and aluminium oxide (Al_2O_3).[5,6] Other thin films, like silicon carbide,[7] titanium oxide,[8,9] aluminium nitride,[10] hafnium oxide,[11–13] and gallium oxide,[14] have also been shown to provide good surface passivation.

Tantalum oxide (Ta_2O_5) is another dielectric compatible with photovoltaic applications, as it has excellent optical properties (i.e., a relatively high refractive index and a negligible absorption in the visible range) to be used as antireflection coating (ARC).[15] In the wider semiconductor industry, Ta_2O_5 has been investigated as an alternative to SiO_2 due to its high dielectric constant, good electrical properties, and relatively high thermal stability.[16] Several different methods for preparing Ta_2O_5 have been explored, such as anodic or thermal oxidation,[17,18] sol-gel deposition,[19] magnetron sputtering,[20,21] atomic layer deposition (ALD),[22,23] and plasma enhanced chemical vapour deposition (PECVD).[24,25] Despite more than four decades of work on Ta_2O_5, no attempt has yet been made to study this material on c-Si as an electronic passivating layer.

This work provides evidence of surface passivation of c-Si by Ta_2O_5 prepared by ALD capped with SiN_x deposited by PECVD. We first present a brief summary of the structural and optical properties of Ta_2O_5 films. We then examine here the passivation quality of Ta_2O_5/SiN_x stacks on several types of c-Si surfaces including *p*-type and *n*-type undiffused, boron-diffused p^+, and phosphorus-diffused n^+. Further, capacitance–voltage (C–V) measurements are undertaken to probe the electronic properties of Ta_2O_5 films before and after SiN_x capping, to elucidate the physical mechanism underlying the evolution in surface passivation.

The Ta_2O_5 films were deposited in a thermal ALD system (R200 Advanced, Picosun) using Tantalum Ethoxide as tantalum precursor, H_2O as the oxidant, and N_2 as the purge gas. The deposition was performed at 250 °C and had a corresponding rate of 0.3 Å/cycle as measured by *ex-situ* spectroscopic ellipsometry (J.A. Woolam M2000 ellipsometer). The film thickness and refractive index *n* were determined by fitting polarized reflectance using Tauc–Lorentz model.[26] The Ta_2O_5 films exhibit $n \sim 2.05$ at 632 nm and negligible absorption of light for wavelengths above 250 nm (~5 eV), that is, for most of the solar spectrum,[27] which confirms their suitability as antireflection coatings. Based on an extensive study into the effect of Ta_2O_5 thickness on surface passivation,[27] a Ta_2O_5 thickness of 12 nm was selected in this work for an optimum passivation quality. X-ray photoelectron spectroscopy performed on the films suggested an approximately stoichiometric Ta_2O_5 film with some trace of metallic tantalum. The stoichiometric composition of Ta_2O_5 is based on the ratio between measured tantalum 4f and oxygen 1 s core level peak areas, scaled by the relevant atomic sensitivity factors.

Cross-sectional transmission electron microscopy (TEM) images were taken with a FEI CM300 system operating at 300 kV to gain insight into the interfacial structure, which is of great importance to surface passivation, as both the recombination-active states and fixed insulator charges are located at or nearby the c-Si interface. The samples were prepared by sectioning double-sided polished wafers, followed by manual grinding and ion milling. Figure 1 presents the TEM image of an as-deposited Ta_2O_5 film, showing an approximate 11 nm thick Ta_2O_5 layer and an approximate 2 nm thick interfacial layer. The interfacial layer may result from (*i*) exposure to air or moisture after DI water rinse, (*ii*) exposure to H_2O during the first few ALD cycles, and/or (*iii*) a more complex reaction between Ta_2O_5 and the c-Si substrate. When the interfacial layer is formed by a reaction

[a]yimao.wan@anu.edu.au

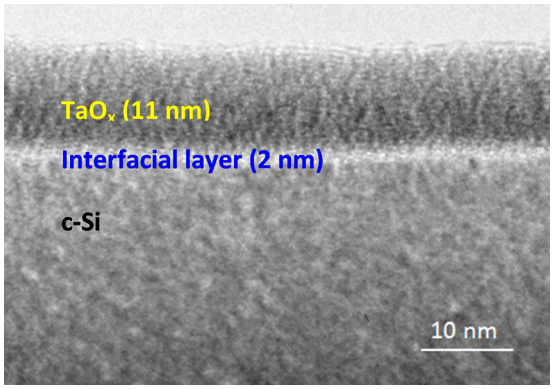

FIG. 1. Cross-sectional TEM image shows an 11 nm as-deposited Ta_2O_5 film with a ~2 nm thick interfacial layer on c-Si.

between the Ta_2O_5 film and c-Si substrate, the layer should have a different bonding configuration from that of pure SiO_2. Alers *et al.*[22] found that the interfacial layer is a composite Si–Ta–O oxide instead of a stoichiometric SiO_2, supported by medium-energy ion scattering results, showing a gradual decrease in atomic density of tantalum across the interfacial layer until undetectable at the surface of c-Si substrate.

To evaluate recombination at the interface between silicon and the deposited dielectrics, symmetrically coated samples were fabricated on four types of c-Si substrates: (*i*) undiffused 0.8 Ω·cm *p*-type wafers (275 μm), (*ii*) undiffused 1.0 Ω·cm *n*-type wafers (390 μm), (*iii*) boron diffused (p^+) 100 Ω·cm *n*-type wafers (280 μm), and (*iv*) phosphorus diffused (n^+) 100 Ω·cm *p*-type wafers (390 μm). All wafers were float-zone (FZ) grown and {100} oriented. The undiffused wafers were etched in tetramethylammonium hydroxide (TMAH, 25 wt. %) at ~ 85 °C to remove saw damage. Boron and phosphorus diffusions were performed in quartz tube furnaces using liquid BBr_3 and $POCl_3$ sources, resulting in sheet resistances of 150 and 120 Ω/sq, as measured by a four-point probe. All samples were then cleaned by the RCA (Radio Corporation of America) procedure and dipped in 1% diluted HF acid to remove any remaining oxide prior to Ta_2O_5 deposition. The capping SiN_x layers were deposited in a microwave/radio-frequency PECVD reactor (AK400, Roth & Rau) at 300 °C. A detailed description of the reactor and deposition conditions is given elsewhere.[28] The capping SiN_x has a thickness of 85 nm and a refractive index of 1.93 at 632 nm. For comparison to well established dielectrics, additional boron and phosphorus diffused samples were coated with ALD aluminium oxide Al_2O_3 and PECVD SiN_x layers, respectively. The deposition details of ALD Al_2O_3 can be found in Ref. 29. The passivating SiN_x was deposited using the same process parameters as those for capping SiN_x.

The effective carrier lifetime τ_{eff} as a function of excess carrier density Δn was measured using a Sinton Instruments WCT-120 photoconductance tool.[30] Neglecting Shockley–Read–Hall recombination in the bulk of the wafer, the upper limit of the effective surface recombination velocity $S_{eff,UL}$ was calculated according to

$$S_{eff,UL} = \frac{W}{2}\left(\frac{1}{\tau_{eff}} - \frac{1}{\tau_{intrinsic}}\right), \quad (1)$$

where W is the c-Si substrate thickness and $\tau_{intrinsic}$ is the intrinsic bulk lifetime of c-Si as parameterized by Richter *et al.*[31] For the heavily diffused p^+ and n^+ c-Si samples, the recombination current density J_0 was extracted from the effective lifetime measurement (taken in transient mode) by employing the technique developed by Kane and Swanson[32] with an intrinsic carrier concentration $n_i = 8.6 \times 10^9\,cm^{-3}$ at 25 °C.

Figure 2 depicts the passivation quality provided by as-deposited and SiN_x-capped Ta_2O_5 films by plotting the injection-dependent effective lifetime τ_{eff} of *p*-type 0.8 Ω·cm and *n*-type 1.0 Ω·cm undiffused c-Si wafers. For reference, $\tau_{intrinsic}$ calculated by the parameterisation given in Ref. 31 is also plotted. As can be seen, the as-deposited Ta_2O_5 provides poor surface passivation on both *p*-type and *n*-type wafers with τ_{eff} around 10 μs at $\Delta n = 10^{15}\,cm^{-3}$. The level of surface passivation is vastly improved by capping the ALD Ta_2O_5 with a PECVD SiN_x layer, resulting in τ_{eff} as high as 1.3 ms and 3.2 ms at $\Delta n = 10^{15}\,cm^{-3}$ on *p*-type and *n*-type c-Si, respectively. These values correspond to an $S_{eff,UL}$ as low as 5.0 cm/s and 3.2 cm/s according to Eq. (1). For comparison, the passivation obtained by SiN_x single layer on identical samples is also plotted in Figure 2. While comparable lifetime was obtained on *p*-type samples by SiN_x and Ta_2O_5/SiN_x stack, the passivation of *n*-type surfaces by SiN_x is slightly better than that by Ta_2O_5/SiN_x stack. Considering the preliminary nature of these results, future process optimisation is expected to improve further the passivation by Ta_2O_5/SiN_x stack.

Moreover, it can be seen for the Ta_2O_5/SiN_x passivated samples that the dependence of τ_{eff} on excess carrier density is relatively constant on *p*-type Si and is considerably injection-dependent on *n*-type Si under low injection conditions (i.e., Δn below $10^{15}\,cm^{-3}$). The behaviour is different to the case of SiN_x, as evidenced in Figure 2, where the lifetime shows an obvious decrease under low excess carrier density on *p*-type Si and remains relatively constant on

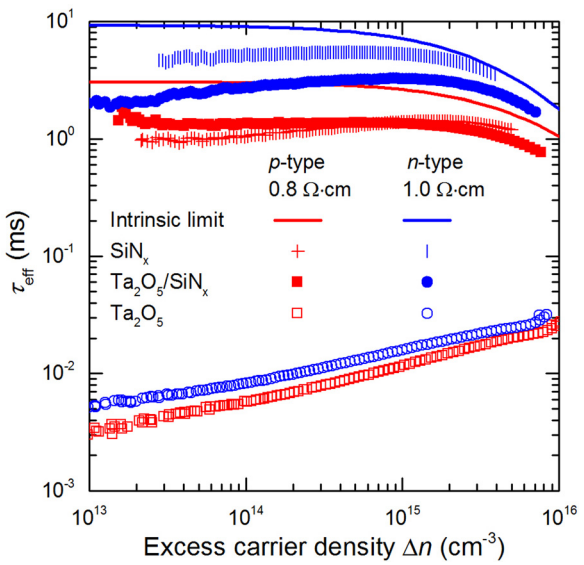

FIG. 2. $\tau_{eff}(\Delta n)$ of FZ *p*-type 0.8 Ω·cm and *n*-type 1.0 Ω·cm undiffused c-Si wafers. The reduction in τ_{eff} at lower Δn for the *n*-type sample is thought to indicate the presence of negative fixed charge in the Ta_2O_5/SiN_x stack.

n-type Si. In addition, this behaviour is commonly observed for Al_2O_3 films, and has been linked to the presence of negative fixed charges in them.[33]

The passivation level provided by the Ta_2O_5/SiN_x stack on boron-diffused surfaces is also found to be very good. Figure 3 plots the Auger-corrected inverse τ_{eff} as a function of excess carrier density of boron-diffused p^+ and phosphorus-diffused n^+ surfaces. It can be seen that the data follow a linear trend, and therefore, we are confident in the accuracy of the extracted J_0 values. For reference, J_0 for thermal ALD Al_2O_3-passivated p^+ and PECVD SiN_x-passivated n^+ samples are also included. As can be seen, the Ta_2O_5/SiN_x stack provides a high level of surface passivation of p^+ surfaces with a J_0 of 25 fA/cm^2, nearly as low as the J_0 attained with Al_2O_3 films (21 fA/cm^2). On the other hand, passivation of the n^+ surface by Ta_2O_5/SiN_x stack appears inferior, exhibiting an approximately 1.5 times higher J_0 than that by SiN_x. The superior passivation of p^+ surfaces over that of n^+ surfaces could again be attributed to the Ta_2O_5/SiN_x stack being negatively charged, although the same behavior could also be explained by surface defects with asymmetric capture cross sections for electrons and holes.

The substantial improvement in surface passivation upon SiN_x capping is fundamentally attributable to one or more of the following causes: (*i*) a reduction in the recombination active defect density at the Ta_2O_5/c-Si interface, (*ii*) an increase in effective fixed charge density, and (*iii*) a reduction in capture cross sections. To evaluate those physical mechanisms, C–V measurements were performed using a 4284 A Precision LCR meter to probe the electronic properties of Ta_2O_5 films before and after SiN_x capping. Double-sided polished *n*-type FZ {100} c-Si with a resistivity of 1.0 Ω·cm and a thickness of 290 μm were coated on one side with a Ta_2O_5 film or a Ta_2O_5/SiN_x stack. The metal–insulator–semiconductor capacitors were fabricated by evaporating aluminium through a shadow mask onto the dielectrics, creating circular dots of diameter ~700 μm and thickness ~100 nm. The rear contact was formed with a GaIn eutectic paste.

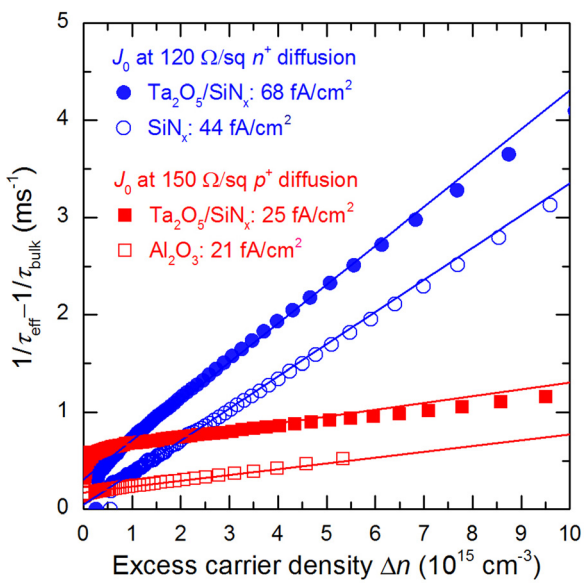

FIG. 3. Auger-corrected inverse $\tau_{eff}(\Delta n)$ of boron-diffused p^+ and phosphorus-diffused n^+ c-Si surfaces when passivated by Ta_2O_5/SiN_x stack, showing the linear fits used to extract J_0. For reference, J_0 for thermal ALD Al_2O_3-passivated p^+ and PECVD SiN_x-passivated n^+ c-Si surfaces are also plotted.

The effective insulator fixed charge density Q_{eff} was calculated from high-frequency C–V measurements by assuming that all charges are located at the Ta_2O_5/c-Si interface. It is worth mentioning that quasistatic C–V measurements on Ta_2O_5 films studied in this work could not be performed, as the thin films exhibit a large leakage current. This leads to an unreliable extraction of mid-gap interface defect density if only based on the high frequency C–V measurements using Terman's method.[34] We therefore were only able to extract the effective charge density Q_{eff}, as shown in Table I. For reference, Q_{eff} of the capping SiN_x ($+0.6\times10^{12}$ cm^{-2}) is also included. This table shows that the as-deposited Ta_2O_5 film possesses a significant amount of negative charge of -1.8×10^{12} cm^{-2}, which is then reduced to -1.0×10^{12} cm^{-2} following SiN_x capping. The substantial improvement in surface passivation upon SiN_x capping is therefore primarily attributable to a reduction in the defect density, presumably via hydrogenation of defects at the Ta_2O_5/c-Si interface during the deposition of SiN_x, rather than to an increase in charge density. Indeed, the charge–assisted passivation is weakened upon SiN_x capping, as evidenced by the decreased negative Q_{eff}.

To further investigate the effect of hydrogenation, we performed two additional experiments. First, single-layer Ta_2O_5 films were annealed in 5% H_2 forming gas at 300 °C for 30 min (i.e., equivalent to the thermal budget of the SiN_x deposition), resulting in a negligible change in surface passivation. Second, equivalent Ta_2O_5 films were capped with 75 nm thick hydrogenated amorphous silicon (a-Si:H) layers deposited by PECVD at 300 °C. Capping with a-Si:H, which has a low fixed charge density (in the order of 10^{10} cm^{-2} as reported by De Wolf *et al.*[35,36]), resulted in a similar passivation quality to capping with SiN_x, with τ_{eff} of 1.1 ms and 2.3 ms on the *p*-type and *n*-type c-Si wafers, respectively. These results suggest that atomic hydrogen released during the SiN_x (or a-Si:H) deposition is essential to achieve a high level of surface passivation, while molecular hydrogen is not sufficient.

In conclusion, we have shown effective passivation of c-Si surfaces by thermal ALD Ta_2O_5 underneath PECVD SiN_x. Surface recombination velocities of 5.0 cm/s and 3.2 cm/s were achieved on *p*-type 0.8 Ω·cm and *n*-type 1 Ω·cm undiffused wafers, respectively. Recombination current densities of 25 fA/cm^2 and 68 fA/cm^2 were measured on 150 Ω/sq p^+ and 120 Ω/sq n^+ c-Si surfaces. C–V measurements revealed that the Ta_2O_5 features negative fixed insulator charge densities of -1.8×10^{12} cm^{-2} and -1.0×10^{12} cm^{-2} before and after capping with PECVD SiN_x. The excellent passivation of both diffused and undiffused *p*-type surfaces

TABLE I. Effective fixed charge density Q_{eff} for capping SiN_x, Ta_2O_5, and Ta_2O_5/SiN_x stack.

	SiN_x	Ta_2O_5	Ta_2O_5/SiN_x
Q_{eff}/q (10^{12} cm^{-2})	0.6 ± 0.05	−1.8 ± 0.24	−1.0 ± 0.14

provided by the negatively charged Ta_2O_5/SiN_x stack is of great interest to current photovoltaics in (*i*) overcoming efficiency limitations imposed by the use of conventional Al-alloyed back surfaces on *p*-type silicon solar cells, and (*ii*) enabling the development of *n*-type silicon solar cells with its concomitant advantages.[37]

We would like to thank Lachlan Black for his assistance in C–V analysis, and thank Mark Hettick for the XPS measurement and analysis. This work has been supported by the Australian government through the Australian Renewable Energy Agency (ARENA) and Trina Solar. Atomic layer deposition and Ellipsometer facilities at the Australian National Fabrication Facility were used in this work. The sample used for cross sectional TEM was prepared in the laboratory at Electronic Materials Engineering, and the imaging was carried out at Centre for Advanced Microscopy.

[1]M. J. Kerr and A. Cuevas, Semicond. Sci. Technol. **17**(1), 35 (2002).
[2]J. Schmidt and M. Kerr, Sol. Energy Mater. Sol. Cells **65**(1–4), 585 (2001).
[3]Y. Wan, K. R. McIntosh, A. F. Thomson, and A. Cuevas, IEEE J. Photovoltaics **3**(1), 554 (2013).
[4]S. De Wolf and M. Kondo, Appl. Phys. Lett. **90**(4), 042111 (2007).
[5]J. Schmidt, A. Merkle, R. Brendel, B. Hoex, M. C. M. van de Sanden, and W. M. M. Kessels, Prog. Photovoltaics: Res. Appl. **16**(6), 461 (2008).
[6]B. Hoex, S. B. S. Heil, E. Langereis, M. C. M. van de Sanden, and W. M. M. Kessels, Appl. Phys. Lett. **89**(4), 042112 (2006).
[7]I. Martín, M. Vetter, A. Orpella, J. Puigdollers, A. Cuevas, and R. Alcubilla, Appl. Phys. Lett. **79**(14), 2199 (2001).
[8]A. F. Thomson and K. R. McIntosh, Prog. Photovoltaics: Res. Appl. **20**(3), 343 (2012).
[9]B. Liao, B. Hoex, A. G. Aberle, D. Chi, and C. S. Bhatia, Appl. Phys. Lett. **104**(25), 253903 (2014).
[10]G. Krugel, A. Sharma, W. Wolke, J. Rentsch, and R. Preu, Phys. Status Solidi RRL **7**(7), 457 (2013).
[11]G. Dingemans and W. M. M. Kessels, ECS Trans. **41**(2), 293 (2011).
[12]J. Wang, S. S. Mottaghian, and M. F. Baroughi, IEEE Trans. Electron Devices **59**(2), 342 (2012).
[13]F. Lin, B. Hoex, Y. H. Koh, J. J. Lin, and A. G. Aberle, Energy Procedia **15**(0), 84 (2012).
[14]T. G. Allen and A. Cuevas, Appl. Phys. Lett. **105**(3), 031601 (2014).
[15]F. Rubio, J. Denis, J. M. Albella, and J. M. Martinez-Duart, Thin Solid Films **90**(4), 405 (1982).
[16]C. Chaneliere, J. L. Autran, R. A. B. Devine, and B. Balland, Mater. Sci. Eng. R **22**(6), 269 (1998).
[17]L. Young, *The Determination of the Thickness, Dielectric Constant, and Other Properties of Anodic Oxide Films on Tantalum from the Interference Colours* (The Royal Society, 1958), p. 41.
[18]D. Mills, L. Young, and F. G. R. Zobel, J. Appl. Phys. **37**(4), 1821 (1966).
[19]J.-Y. Zhang, L.-J. Bie, V. Dusastre, and I. W. Boyd, Thin Solid Films **318**(1–2), 252 (1998).
[20]X. M. Wu, P. K. Wu, T.-M. Lu, and E. J. Rymaszewski, Appl. Phys. Lett. **62**(25), 3264 (1993).
[21]S. Seki, T. Unagami, and B. Tsujiyama, J. Electrochem. Soc. **131**(11), 2621 (1984).
[22]G. B. Alers, D. J. Werder, Y. Chabal, H. C. Lu, E. P. Gusev, E. Garfunkel, T. Gustafsson, and R. S. Urdahl, Appl. Phys. Lett. **73**(11), 1517 (1998).
[23]K. Kukli, J. Aarik, A. Aidla, O. Kohan, T. Uustare, and V. Sammelselg, Thin Solid Films **260**(2), 135 (1995).
[24]J. L. Autran, P. Paillet, J. L. Leray, and R. A. B. Devine, Sens. Actuators A **51**(1), 5 (1995).
[25]D. Laviale, J. C. Oberlin, and R. A. B. Devine, Appl. Phys. Lett. **65**(16), 2021 (1994).
[26]G. E. Jellison, Jr. and F. A. Modine, Appl. Phys. Lett. **69**(3), 371 (1996).
[27]Y. Wan, J. Bullock, and A. Cuevas, "Passivation of c-Si surfaces by ALD tantalum oxide capped with PECVD silicon nitride," Sol. Energy Mater. Sol. Cells (submitted).
[28]Y. Wan, K. R. McIntosh, and A. F. Thomson, AIP Adv. **3**(3), 032113 (2013).
[29]W. Liang, K. J. Weber, S. Dongchul, S. P. Phang, Y. Jun, A. K. McAuley, and B. R. Legg, IEEE J. Photovoltaics **3**(2), 678 (2013).
[30]R. A. Sinton and A. Cuevas, Appl. Phys. Lett. **69**(17), 2510 (1996).
[31]A. Richter, S. W. Glunz, F. Werner, J. Schmidt, and A. Cuevas, Phys. Rev. B **86**(16), 165202 (2012).
[32]D. Kane and R. M. Swanson, presented at the 18th IEEE Photovoltaic Specialists Conference, Las Vegas, USA, 1985.
[33]B. Veith, T. Ohrdes, F. Werner, R. Brendel, P. P. Altermatt, N.-P. Harder, and J. Schmidt, Sol. Energy Mater. Sol. Cells **120**, 436–440 (2013).
[34]L. M. Terman, Solid-State Electron. **5**(5), 285 (1962).
[35]S. De Wolf, C. Ballif, and M. Kondo, Phys. Rev. B **85**(11), 113302 (2012).
[36]S. De Wolf, B. Demaurex, A. Descoeudres, and C. Ballif, Phys. Rev. B **83**(23), 233301 (2011).
[37]D. Macdonald and L. J. Geerligs, Appl. Phys. Lett. **85**(18), 4061 (2004).